

## Paper

Int'l J. of Aeronautical & Space Sci. 17(3), 341–351 (2016)  
DOI: <http://dx.doi.org/10.5139/IJASS.2016.17.3.341>

# Effect Of Hole Shapes, Orientation And Hole Arrangements On Film Cooling Effectiveness

**Prakhar Jindal\***, **A.K. Roy\*\*** and **R.P. Sharma\*\*\***

*Department of Mechanical Engineering, Birla Institute of Technology, Mesra, Ranchi, JH 835215, India.*

## Abstract

In this present work, the effect of hole shapes, orientation and hole arrangements on film cooling effectiveness has been carried out. For this work a flat plate has been considered for the computational model. Computational analysis of film cooling effectiveness using different hole shapes with no streamwise inclination has been carried out. Initially, the model with an inclination of 30° has been verified with the experimental data. The validation results are well in agreement with the results taken from literature. Five different hole shapes viz. Cylindrical, Elliptic, Triangular, Semi-Cylindrical and Semi-Elliptic have been compared and validated over a wide range of blowing ratios. The blowing ratios ranged from 0.67 to 1.67. Later, orientation of holes have also been varied along with the number of rows and hole arrangements in rows. The performance of film cooling scheme has been given in terms of centerline and laterally averaged adiabatic effectiveness. Semi-elliptic hole utilizes half of the mass flow as in other hole shapes and gives nominal values of effectiveness. The triangular hole geometry shows higher values of effectiveness than other hole geometries. But when compared on the basis of effectiveness and coolant mass consumption, Semi-elliptic hole came out to give best results.

**Key words:** CFD, Film cooling, hole shapes, blowing ratio, effectiveness, Orientation.

## Nomenclature

$T_{\infty}$	Free stream temperature, K
$T_{aw}$	Adiabatic wall temperature, K
$T_c$	Coolant temperature, K
$\eta$	Adiabatic cooling effectiveness, $\frac{T_{\infty} - T_w}{T_{\infty} - T_c}$
$M$	Mass flux ratio or blowing ratio (defined as ratio of mass flux of coolant to the mainstream)
$\theta$	Non-dimensional Temperature, $\frac{T_H - T_w}{T_H - T_c}$

## 1. Introduction

The thermal management and protection of the components and surfaces in rocket engine combustion chambers presents one of the most challenging problems for

designers. Film cooling is an active cooling strategy, which involves the continuous injection of a thin layer of protective fluid (coolant) near a wall or boundary to insulate it from rapidly flowing hot propellant gases. Its main advantages are that it allows for the use of much lighter-weight nozzle assemblies and it is relatively simple to implement from a fabrication standpoint.

Film cooling is usually measured in dimensionless form known as “film cooling effectiveness”, and defined as:

$$\eta = \frac{T_{\infty} - T_w}{T_{\infty} - T_c} \quad (1)$$

where,  $T_w$  is adiabatic wall temperature,  $T_{\infty}$  is freestream temperature = 600 K, &  $T_c$  is coolant inlet temperature = 300 K

To study film cooling phenomena, investigators have been using simple geometries to reduce the complexity of the flow affecting the heat exchange between the test surface and the mainstream gas flow. The geometrically simple form of

This is an Open Access article distributed under the terms of the Creative Commons Attribution Non-Commercial License (<http://creativecommons.org/licenses/by-nc/3.0/>) which permits unrestricted non-commercial use, distribution, and reproduction in any medium, provided the original work is properly cited.

© \* Ph. D Student, Corresponding author: prakharj@bitmesra.ac.in  
\*\* Associate Professor  
\*\*\* Professor

a flat plate with one or more film cooling holes often offers a sufficient approximation of the reality for a lot of research interests. A better understanding of the mechanisms involved in film cooling is needed to achieve an optimized and effective film cooling with a minimum amount of coolant. However, the effectiveness of film cooling is very much dependent on the shape of the injection hole, layout geometry and injection angle [1].

Many researchers have conducted computational and experimental work on film cooling, some of which can be found here. Bunker [2] in his comprehensive review paper on film cooling from shaped holes has pointed out that no single shaping of film hole stands as an optimal geometry for all applications. He also concluded that hole shape maintains the cooling jets closer to surface, enhances film coverage and reduces mixing. Goldstein et al. [3-4] reported the effectiveness resulting from a single cylindrical hole and row of holes. They considered a blowing ratio ( $M$ ) of 0.5 for maximum effectiveness at coolant to freestream DR (Density Ratio) around 1.0. Film cooling effectiveness using a cylindrical hole at an angle of  $30^\circ$ ,  $60^\circ$  and  $90^\circ$  was studied by Yuen and Martinez [5]. They considered a hole length of  $L=4D$ , the free-stream Reynolds number of 8563 based on the free-stream velocity and hole diameter, and the blowing ratio was varied from 0.33-2. For a single  $30^\circ$  hole, the maximum effectiveness increased up to a blowing ratio of 0.5, then decreased with increasing blowing ratio due to jet penetration into the free stream. Yuen and Martinez [6] in their another paper studied the film cooling effectiveness and heat transfer coefficients for a rows of round holes with different hole inclinations. To study the effect of injecting a small amount of water into the cooling air for film cooling performance, FLUENT was used by T. Wang and X. Li [7]. Their operating conditions were a pressure of 15 atm and a temperature of 1561K. The result showed that 5-10% cooling effectiveness was achieved by 10-20% mist. Influence of different hole shapes on film cooling with  $CO_2$  was investigated by G. Li et al. [8].

Concluding from the literatures, film cooling effectiveness mainly depends on certain factors such as blowing ratio, injection angle, compound angle/orientation,  $L/D$  ratio etc. Hence, the present work aims to further investigate the effects of different coolant hole geometries with varying lateral orientations of the holes on the flow structure for a flat plate in FLUENT using  $k-\epsilon$  turbulence model. To achieve this objective, multiple computations has been conducted for different hole geometries and for more number of rows with aligned and staggered hole configurations at several blowing ratios ranging from 0.67 to 1.67. Compound angles of the holes have also been varied from  $0^\circ$  to  $90^\circ$ .

## 2. Computational Modelling

### 2.1 Physical Model

GAMBIT 2.4.6 has been used to model the computational domain and also to generate mesh. In the present study,  $k-\epsilon$  turbulence model has been used. The hot combustion gases are passing over the surface of a flat plate and the coolant is being injected to create a film above it. The inclination of coolant injection is  $30^\circ$  and the compound angle is varied from  $0^\circ$  to  $90^\circ$ . Validation of the model has been done using the results of cylindrical cooling hole with the experimental study of Yuen et al. [5]. The geometrical conditions have been kept in coordination with the literature work so as to achieve better validation results. In the later part of the study, three different shaped holes (semi-cylindrical, semi-elliptic and triangular) have been investigated. The cross-sectional area of other hole configurations used in this work has been kept same as that of cylindrical hole. Fig. 1 shows the computational domain along with the dimensions and the boundary conditions. Fig. 2 shows the compound angles of the hole shapes while Fig. 3 shows the geometry of all the hole shapes used.

### 2.2 Boundary Conditions

For validation, the geometry consists of a single cylindrical

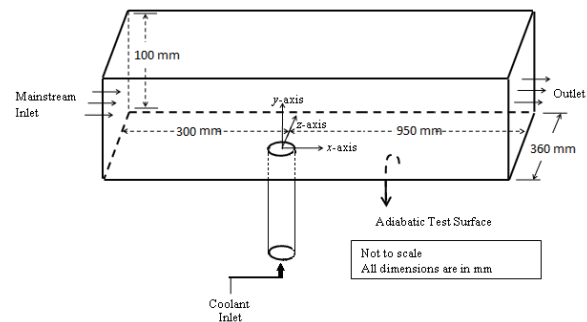


Fig. 1. Geometry of Computational Domain

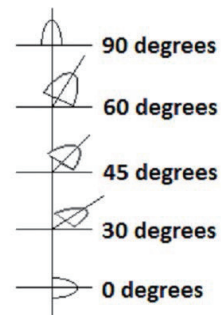


Fig. 2. Compound Angles used for the Hole Shapes

hole inclined at an angle of 30° streamwise having hole diameter 10mm. The L/D ratio is 7. Reynolds number based on freestream velocity and hole diameter is 10364. Blowing ratios ranging from 0.67 - 1.67 have been investigated which corresponds to the coolant inlet velocities (Table 2). Table 1 gives the values of boundary conditions used.

For grid dependency, the cylindrical hole case for blowing ratio M=0.33 is selected. Different meshes have been tried. Fig. 4 shows the mesh dependency for centerline effectiveness. The different grid size for various meshes is tabulated in the Table 3. From Fig. 4 it is clear that the result in case of medium 2 and fine meshes are almost similar but still fine mesh is

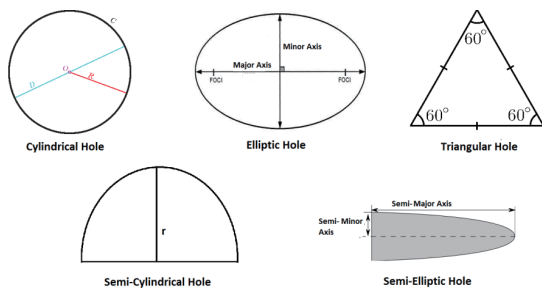


Fig. 3. Geometry of Each Hole Shapes

Table 1. Boundary Conditions

Conditions	Values
Mainstream Inlet Velocity	15m/s
Mainstream Inlet Temperature	600 K
Density Ratio	1 (approx.)
Coolant Inlet Temperature	300 K

Table 2. Coolant Inlet Velocities with blowing ratios

S.No.	Blowing Ratio (M)	Coolant Inlet Velocity
1.	0.67	10 m/s
2.	1.00	15 m/s
3.	1.33	20 m/s
4.	1.67	25 m/s

Table 3. Different grid size for various meshes

Grid	Cells	Faces	Nodes
Coarse 1	153459	477210	165291
Coarse 2	328161	1012327	347496
Medium 1	634220	1946355	664793
Medium 2	1218504	3722716	1265080
Fine	3818610	11548110	3911869

used for analysis to achieve more accurate results.

2.2.1. Solver

A 3D segregated, steady state solver was used. For linearization of governing equations implicit method was used. For turbulence modeling k-ε model with standard wall functions was used. To avoid use of enhanced wall treatment mesh was kept fine enough to have wall Y+ in the range 0-5. Discretization scheme used was in 2nd order upwind for momentum, turbulence kinetic energy, turbulence dissipation rate and energy, whereas for pressure standard discretization scheme was used [9]. For pressure-velocity coupling SIMPLE algorithm was used. A UDF was used for plotting the centerline effectiveness in all the cases. Convergence is considered to be achieved when the residual values are less than 10<sup>-5</sup> for continuity equation, 10<sup>-7</sup> for momentum and 10<sup>-8</sup> for energy.

2.2.2. Governing Equations

The continuity (2) and momentum (3) equations for the present case of steady state, incompressible, segregated 3D solver and standard k-ε (without viscous heating) turbulence model are:

$$\frac{\partial u_i}{\partial x_i} = 0 \tag{2}$$

$$\frac{\partial}{\partial x_j} (\rho u_i u_j) = -\frac{\partial p}{\partial x_i} + \frac{\partial}{\partial x_j} \left[ \mu \left( \frac{\partial u_i}{\partial x_j} + \frac{\partial u_j}{\partial x_i} - \frac{2}{3} \delta_{ij} \frac{\partial u_k}{\partial x_k} \right) \right] + \frac{\partial}{\partial x_j} (-\rho \bar{u}'_i \bar{u}'_j) \tag{3}$$

where,

$$-\rho \bar{u}'_i \bar{u}'_j = \mu_t \left( \frac{\partial u_i}{\partial x_j} + \frac{\partial u_j}{\partial x_i} \right) - \frac{2}{3} \left( \rho \kappa + \mu_t \frac{\partial u_k}{\partial x_k} \right) \delta_{ij} \tag{4}$$

The two additional transport equations (for the turbulence kinetic energy, *k*, and the turbulence dissipation rate, *ε*, are solved, and μ<sub>t</sub> (turbulent viscosity) is computed as a function of *k* and *ε* as:

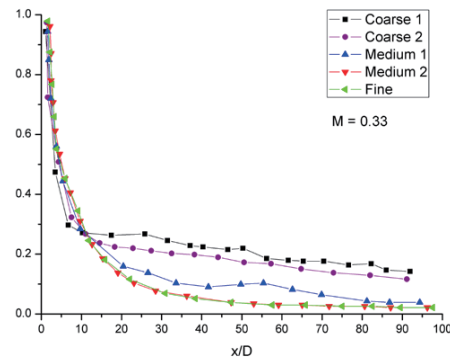


Fig. 4. Grid Dependency Test

$$\rho \frac{\partial}{\partial x_j} (k u_i) = \frac{\partial}{\partial x_j} \left[ \left( \mu + \frac{\mu_t}{\sigma_k} \right) \frac{\partial k}{\partial x_j} \right] + G_k - \rho \varepsilon \tag{5}$$

$$\rho \frac{\partial}{\partial x_j} (\varepsilon u_i) = \frac{\partial}{\partial x_j} \left[ \left( \mu + \frac{\mu_t}{\sigma_\varepsilon} \right) \frac{\partial \varepsilon}{\partial x_j} \right] + C_{1\varepsilon} \frac{\varepsilon}{\kappa} G_k - C_{2\varepsilon} \rho \frac{\varepsilon^2}{k} \tag{6}$$

$$\mu_t = \rho C_\mu \frac{k}{\varepsilon} \tag{7}$$

The model constants known as the turbulent Prandtl number for  $k$  is taken as  $\sigma_k = 1.0$  and the model constant known as turbulent Prandtl number for  $\varepsilon$  is used as  $\sigma_\varepsilon = 1.3$  along with the model constant  $C_{1\varepsilon}$ ,  $C_{2\varepsilon}$  and  $C_\mu$  taken as the default values ( $C_{1\varepsilon} = 1.44$ ,  $C_{2\varepsilon} = 1.92$  and  $C_\mu = 0.09$ ) in FLUENT. As these model constant values are standard one and have been found to work fairly well with wide range of wall bounded and free shear flows, hence the same are used for the present computational model [10].

### 3. Results and Discussion

#### 3.1 Validation - Cylindrical Hole(Single)

For the validation of the turbulence model used, the computational results obtained for the case of cylindrical holes have been verified by the experimental data of Yuen et al. [5]. The performance of different hole shapes (Semi-cylindrical, semi-elliptic and triangular) for film cooling effectiveness has been measured in terms of centerline and spatially averaged adiabatic film cooling effectiveness.

Also the non-dimensional temperature profiles have been plotted for all the cases. Figure 5 shows the validation of computational results with the experimental data. The given Fig. 5 shows validation for all the blowing ratios. As can be seen from the Fig. 5, the centerline effectiveness is very much in agreement with the experimental results throughout the length except in the near hole region ( $x/D < 5.0$ ). This sudden decrease of effectiveness is might be a result of mainstream penetration into coolant jet or may be due to coolant jet lift-off from the adiabatic surface.

The immediate decrease of effectiveness in near hole region is may be due to the penetration of mainstream fluid into the coolant jet while for blowing ratios 0.67 and 1.0, due to the jet lifting-off from the surface the centerline effectiveness decreases to very low values in the near hole region. Also, the results are much in agreement with the experimental results for the cases of B.R. 1.0 and above, as the model used is  $k-\varepsilon$  which is usually employed for flows having high Reynolds number. For near wall flows  $k-\varepsilon$  model can be employed which might give better results for low B.R. ( $< 1.0$ ).

#### 3.2 Effect of Hole Shapes v/s Blowing Ratios

The Figures (6-9) below depict the centreline film cooling effectiveness from semi-cylindrical, elliptic, semi-elliptic and triangular holes along with full cylindrical hole. In all the cases, triangular hole shape gave the

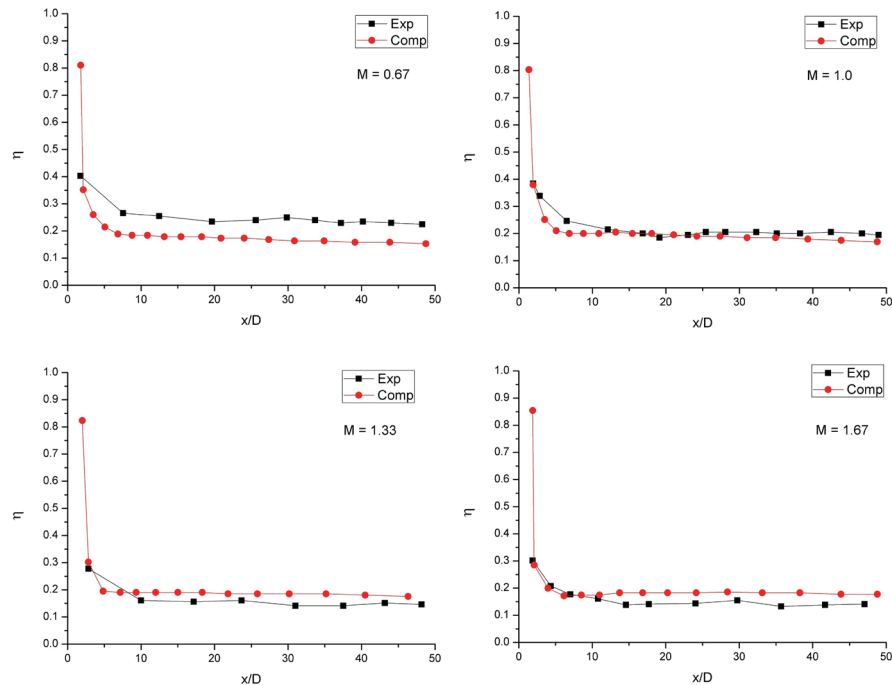


Fig. 5. Centerline effectiveness for individual case of blowing ratios (M) for cylindrical hole shapes

best result for effectiveness but on the other hand, both the semi-geometries gave better results than the full cylindrical hole. For the low blowing ratio cases (0.67, 1.0), the centreline effectiveness values are much higher for semi-elliptic and triangular cases rather than other hole shapes (Figs. 6, 7).

The semi-cylindrical hole shape has almost same values of effectiveness as that of full cylindrical hole. For higher blowing ratios of 1.33, 1.67 (Figs. 8, 9), in the near hole region, the effectiveness values are slightly higher in the case of both semi-geometries and triangular holes than that of cylindrical hole. Although, the triangular hole shape is giving better values of effectiveness in all the cases but semi-elliptic hole will have an upper hand as it utilizes half the coolant mass flow rate per unit area as that of triangular hole.

Spatially averaged film cooling effectiveness for different hole shapes have been plotted (Fig. 10) to see the effect of blowing ratios and geometries. For the case of cylindrical and semi-cylindrical hole shape, the effectiveness values decrease up to  $M = 1.0$  while for the others, the value keeps on decreasing until  $M = 1.33$ . Among all the shapes, triangular hole shows highest values of spatially averaged effectiveness,

but when it comes to coolant mass flow consumption then the semi-elliptic hole is way above both semi-cylindrical and cylindrical hole shapes.

For explaining the concept of jet heights, non-dimensional temperature profiles are plotted. For higher effectiveness values less jet heights are desirable. As can be seen from the Figs. 11-14, both the semi-geometries have less jet heights and hence have higher effectiveness values. In the Figure  $\theta = 0.0$  implies to freestream temperature (600K) while  $\theta = 1.0$  implies to coolant temperature (300K) without any mixing of the freestream. Inferring from Fig. 11, semi-elliptic hole have least jet mean height while full cylindrical hole has maximum jet height and hence vice-versa for the effectiveness values. The coolant jet height was found to be increasing with increasing blowing ratios. Also, no coolant was found above the  $y/D$  value of 2.5.

Similar trend of the curve can be seen for other blowing ratios ( $M = 1.0$  to 1.67) in Figs. 12-14. The semi-elliptic hole showed least jet mean height while full cylindrical hole showed maximum jet height and hence vice-versa for the effectiveness values. Hence the Semi-elliptic hole came out to be the best based on jet mean heights and hence for the effectiveness.

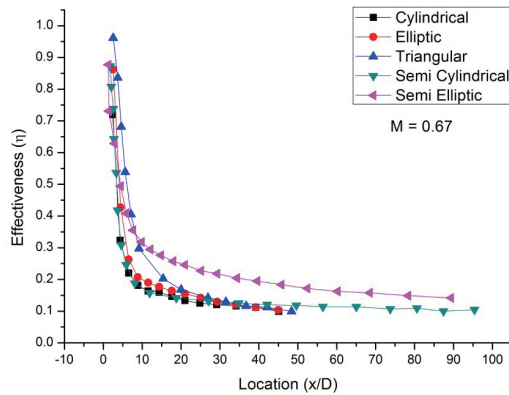


Fig. 6.  $\eta$  for Different Hole Shapes at  $M = 0.67$

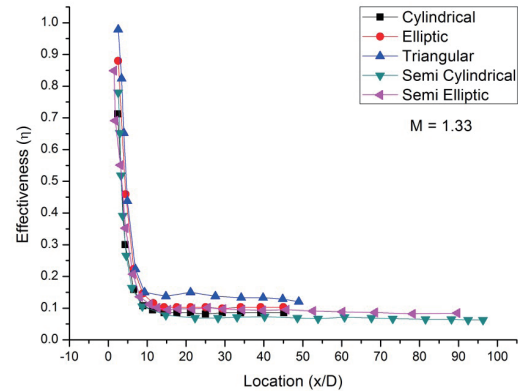


Fig. 8.  $\eta$  for Different Hole Shapes at  $M = 1.33$

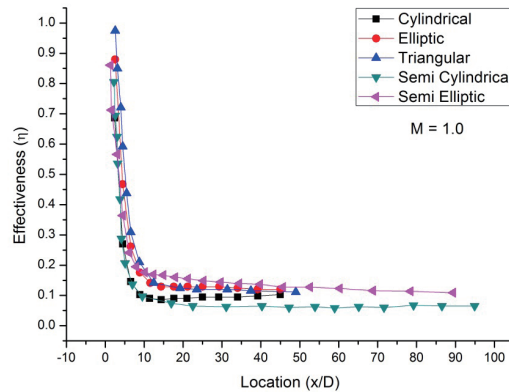


Fig. 7.  $\eta$  for Different Hole Shapes at  $M = 1.0$

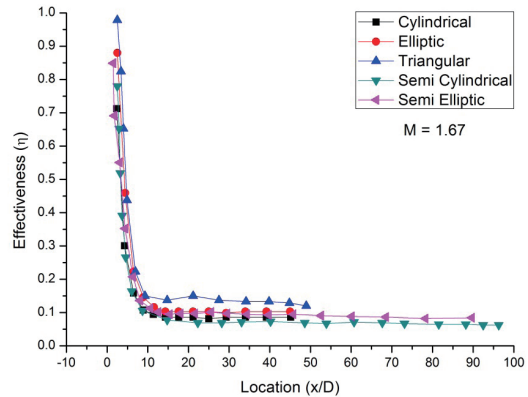


Fig. 9.  $\eta$  for Different Hole Shapes at  $M = 1.67$

### 3.3 Arrangement of Holes/Rows

Since the coolant mass flow rate is half for the semi-geometries cases, they have been preferred over triangular hole for introducing coolant from multiple rows of holes. Fig. 15 shows the arrangement of row of holes for single row, 2 inline rows and 2 staggered row arrangements.

The comparative results of single row of cylindrical holes with two aligned rows of semi-elliptic and two staggered rows of semi-elliptic holes have been shown in the Figs. 16, 17 and 18. As it was the case for single hole, both semi-geometric hole shapes have higher values of centreline effectiveness at all  $x/D$  values for all blowing ratios (1.0, 1.33, 1.67).

In the near hole region, there is a sudden decrease of effectiveness which might be due to coolant jet lift-off. Since

the decrement of the effectiveness is minimum for staggered row case as compared to others, so the jet lift-off is minimum.

Up till  $x/D < 10$ , the centreline values for aligned semi-elliptic rows is higher at blowing ratios 1.0 and 1.33. This might be because of the continuous support of coolant from upstream row. Apart from this, at all other  $x/D$  values ( $> 10$ ), staggered rows of holes have much higher effectiveness values. This is mainly because the coolant is widely spread on the surface and there was no space left for the freestream flow to enter in between holes of downstream staggered row. Also for the staggered case the reattachment of jet to the plate surface started at around  $x/D = 7$  as compared to others. This may be because of the arrangement of holes as the lateral distance between the holes of both the rows is governed by each other.

The Fig. 19 shows the spatially averaged effectiveness for

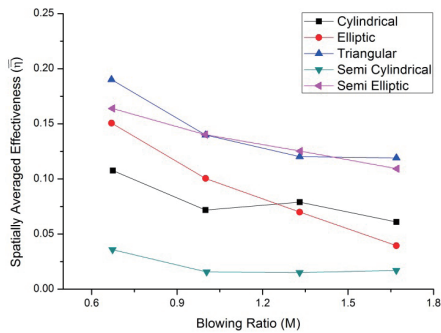


Fig. 10. Variation of  $\bar{\eta}$  with Blowing Ratios

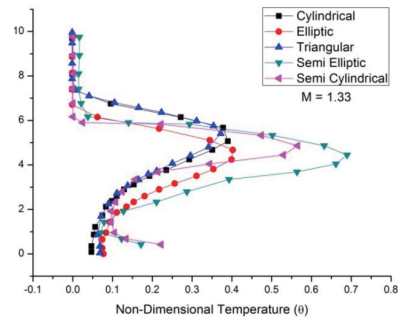


Fig. 13. Variation of  $\theta$  with  $y/D$  for all shapes at  $M = 1.33$

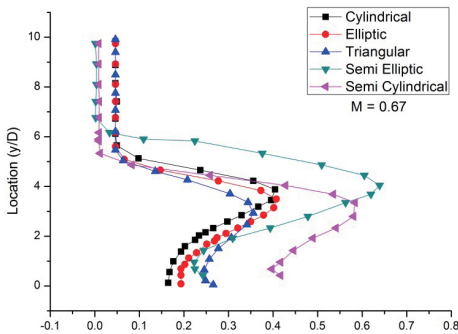


Fig. 11. Variation of  $\theta$  with  $y/D$  for All Shapes at  $M = 0.67$

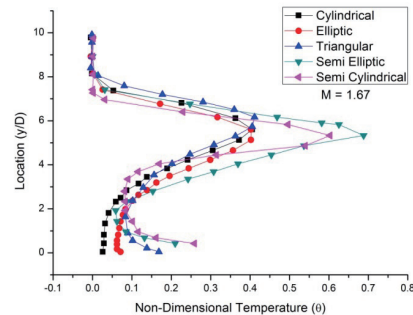


Fig. 14. Variation of  $\theta$  with  $y/D$  for All Shapes at  $M = 1.67$

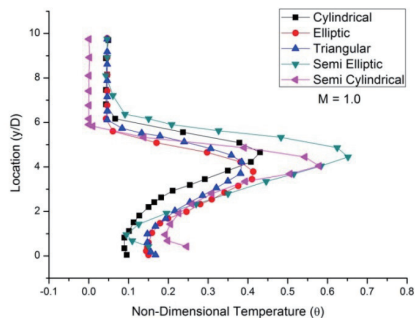


Fig. 12. Variation of  $\theta$  with  $y/D$  for All Shapes at  $M = 1.0$

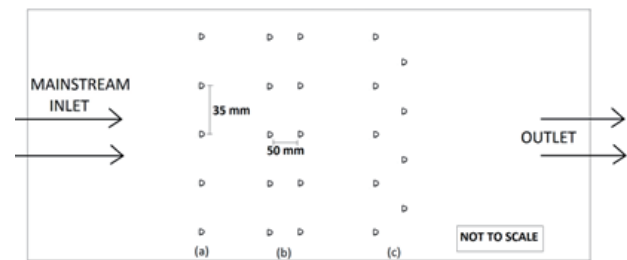


Fig. 15. Arrangements of row of holes (a) Single Row (b) 2 Inline Row (c) 2 Staggered Row

all hole configurations at all blowing ratios. The spatially averaged effectiveness for one row of full cylindrical hole and semi-cylindrical hole is almost similar and well below others. For the case of two rows of staggered semi-elliptic holes, the effectiveness values are almost twice of the values of the single row of cylindrical holes.

The non-dimensional temperature profile for all hole configurations have been plotted at all blowing ratios. The

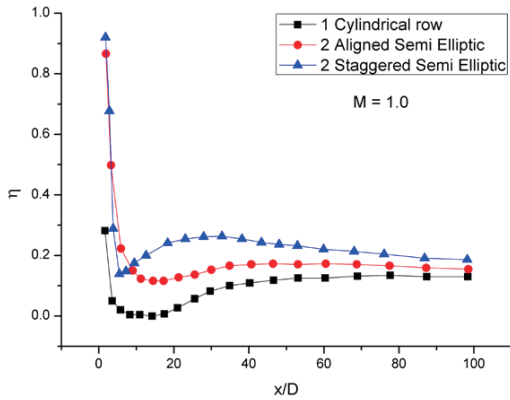


Fig. 16.  $\eta$  for Multiple Row of Holes at  $M = 1.0$

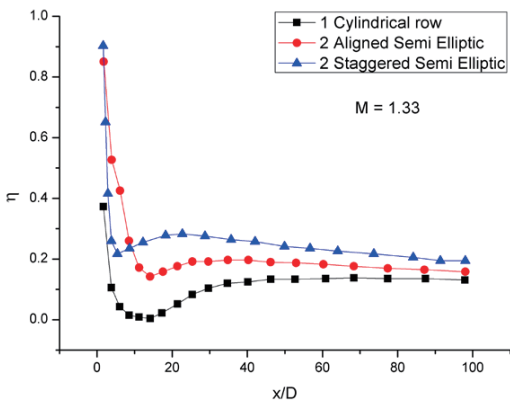


Fig. 17.  $\eta$  for Multiple Row of Holes at  $M = 1.33$

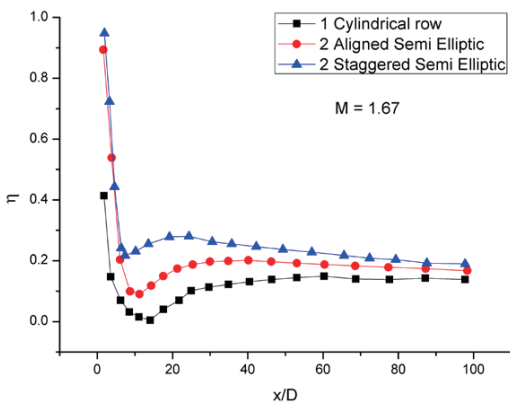


Fig. 18.  $\eta$  for Multiple Row of Holes at  $M = 1.67$

notations  $\theta$  at 0.0 and at 1.0 have the same meaning as mentioned in the above section. The maximum  $\theta$  value at a particular location gives the mean jet height of the coolant at that point. It is seen from all the cases that the coolant jet height increases with the increase of blowing ratio. The Fig. 20, shows the different coolant hole configurations at  $M = 1.0$  only. It is very clear from the Figure (20) that the mixing of coolant into the freestream flow is least for the semi-geometry row cases as they have much lower jet heights than the row of cylindrical holes. The semi-elliptic two staggered rows show the minimum coolant jet heights and hence they have maximum effectiveness values for all the cases. At low  $y/D$  values, the presence of coolant is very high as can be seen from high  $\theta$  values for all semi-elliptic cases.

### 3.4 Compound Angle Orientations

In this section, all the different hole configurations for single and multiple rows have been compared at fixed values of orientation angle ( $\beta$ ) which is varied from  $0^\circ$  to  $90^\circ$ . One row of cylindrical holes has been compared with the two staggered rows of semi-cylindrical and semi-elliptic holes at

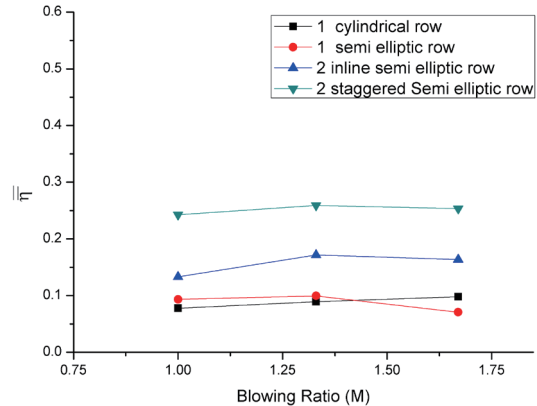


Fig. 19. Variation of  $\bar{\eta}$  with Blowing Ratios

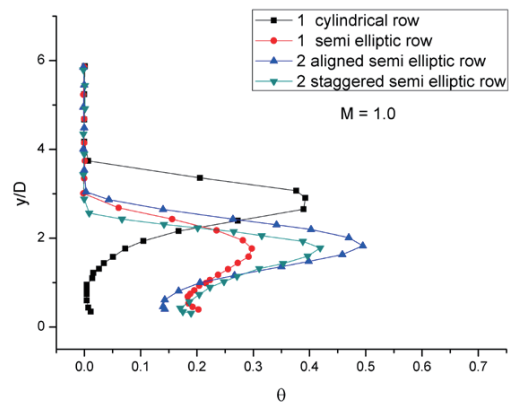


Fig. 20. Variation of  $\theta$  with  $y/D$  for Multiple Rows

blowing ratio 1.0. The P/D ratio for cylindrical holes and for semi-geometric holes is 5. Much higher values of centreline effectiveness have been achieved at all the compound angles for staggered rows of semi-geometric holes than the single row of cylindrical holes. While comparing in between the staggered rows of semi-geometric holes, the semi-elliptic holes steals the show with much higher effectiveness values than other two configurations.

As can be seen from the Fig. 21 for  $\beta = 0^\circ$ , there is a sharp increase in the effectiveness just after the near hole region which might be a result of sudden reattachment of coolant jet with the surface. For  $\beta = 30^\circ$  Fig. 22, the effectiveness for the semi elliptic case is much higher at  $8 \leq x/D \leq 25$ .

But for both the semi-geometries, the effectiveness values are higher than that of cylindrical row of holes. On comparing the results of  $\beta = 30^\circ$  to  $\beta = 0^\circ$  one can infer that the difference in the effectiveness has been reduced.

For  $\beta = 45^\circ$ , the semi-cylindrical row of holes show higher effectiveness than the other two configurations of row of holes in the streamwise region of  $15 \leq x/D \leq 100$  (Fig. 23). However, from Fig. 24, for  $\beta = 60^\circ$  both the staggered rows of semi geometries have almost same effectiveness values but

have far increased value of effectiveness than the cylindrical row of holes.

From Fig. 25, at  $\beta = 90^\circ$ , the centreline effectiveness from each case of staggered rows of semi geometric holes is much higher than that of the cylindrical holes after the streamwise region of  $1 \leq x/D \leq 5$ . Again, the semi-elliptic hole shape gives much higher values of effectiveness upto  $x/D = 25$  after which it becomes almost equal to the values from semi-cylindrical case.

The spatially averaged effectiveness have been plotted for all the hole configurations at all orientation angles and is shown in Fig. 26. The effectiveness increases with increase in  $\beta$  upto  $60^\circ$  for cylindrical and semi-cylindrical case while it decreases on further increasing the angle. For semi-elliptic holes, the effectiveness decreases with increase in orientation angle upto  $30^\circ$  and an insignificant increase till  $45^\circ$ , while it further increases with increase in the angle. At  $\beta = 0^\circ$  the two staggered semi-elliptic holes show much higher effectiveness than the other two configurations. There is a significant increase of about 400% in the spatially averaged effectiveness from rows of semi-elliptic holes than the row of cylindrical holes.

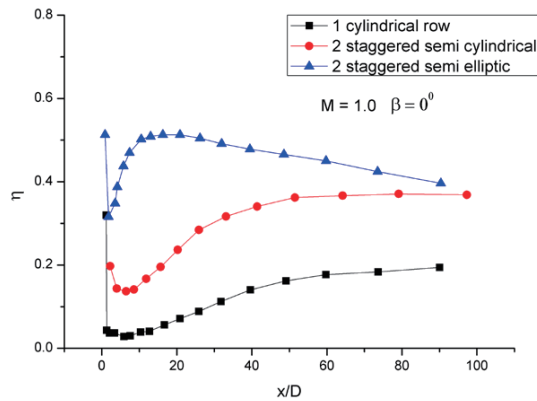


Fig. 21.  $\eta$  for Multiple Rows with  $\beta = 0^\circ$

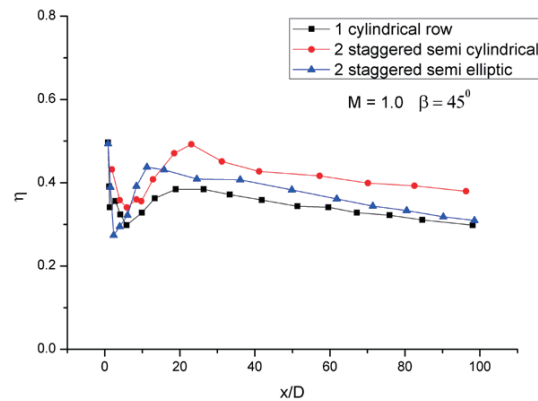


Fig. 23.  $\eta$  for Multiple Rows with  $\beta = 45^\circ$

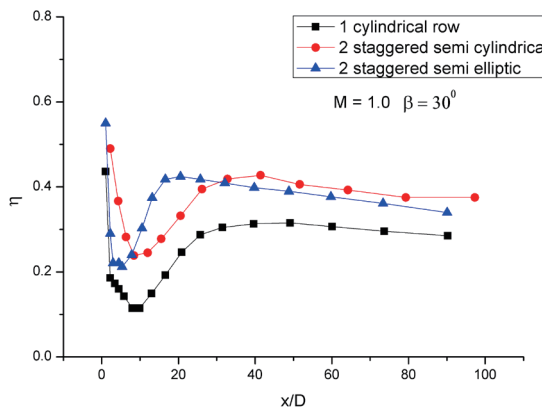


Fig. 22.  $\eta$  for Multiple Rows with  $\beta = 30^\circ$

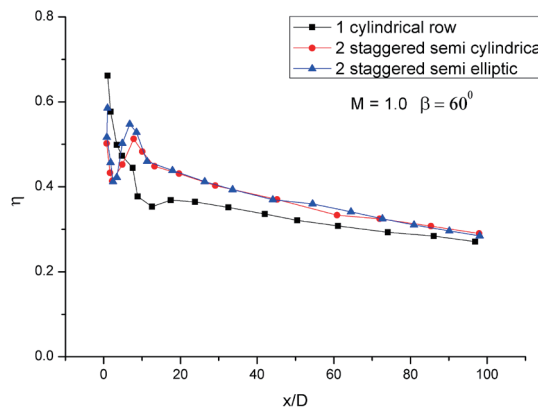


Fig. 24.  $\eta$  for Multiple Rows with  $\beta = 60^\circ$

### 4. Effectiveness Profile for Various Holes Shapes & Their Orientations

The phenomenon of effectiveness, discussed in the previous sections of the paper, has been represented using the contour of effectiveness in the Fig. 27. The effectiveness contours have been presented for four blowing ratios (0.67–1.67) for all the hole shapes described as (a – e). As can be seen from Fig. 27, the centerline film cooling effectiveness was found to be maximum at the blowing ratio of 1.0 for the triangular and semi-elliptic hole shapes closely followed by the elliptic hole shape. While the semi-cylindrical and cylindrical hole shapes was found to be ineffective for the enhancement of film cooling effectiveness at all blowing ratios as quoted in the previous sections. From the contours, the effectiveness was found to be increasing for the blowing ratio 0.67 to 1.0 and then it further decreases from 1.0 to 1.67.

The reason behind higher film cooling effectiveness from the triangular and semi-elliptic hole among other hole shapes might be less jet heights and better lateral spreading resulting in the formation of a uniform coverage film over the surface. Also the geometry of the triangular hole might be allowing

to distant lateral spreading, further adding to the increased effectiveness values. This can be verified by plotting a temperature contour for the cylindrical, triangular and semi-elliptic hole shapes. Fig. 28 shows the temperature contours on a cross-plane downstream of the location of coolant jet inlet. In the case of cylindrical hole on the lower chamber wall surface, the temperature distribution is governed by the coolant jet and its interaction with the mainstream flow which rather shows a conventional distribution with a low temperature core and gradually increasing flow temperature away from the core.

The spread of this low temperature region in both the directions indicate a lower lateral spreading and less effectiveness. In the case with semi-elliptic hole, a broad low temperature region is seen with gradually increasing flow temperature up to the mainstream value. The temperature in the flow core with the triangular hole is much lesser as compared to those in the core of cylindrical hole case, indicating the higher cooling effects produced by the triangular hole. The spread of this low temperature region indicated by the arrows drawn on the contour further indicate the lateral spreading of the jet and the effective lower wall surface interacting with the cool flow. The low temperature coolant flow in the Triangular and Semi-elliptic hole case interacts with a wider region of lower chamber wall

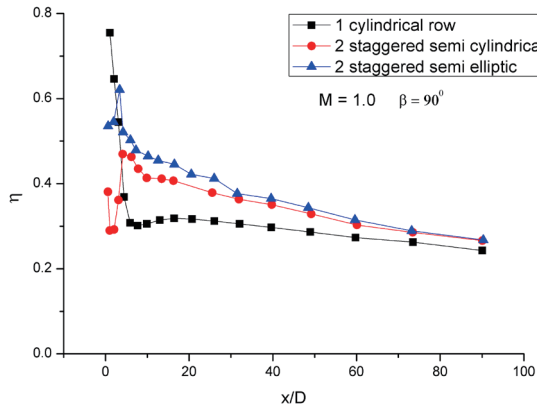


Fig. 25.  $\eta$  for Multiple Rows with  $\beta = 90^\circ$

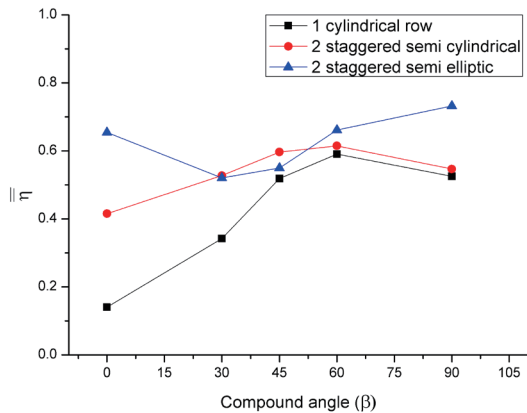


Fig. 26. Variation of  $\eta$  with Blowing Ratios

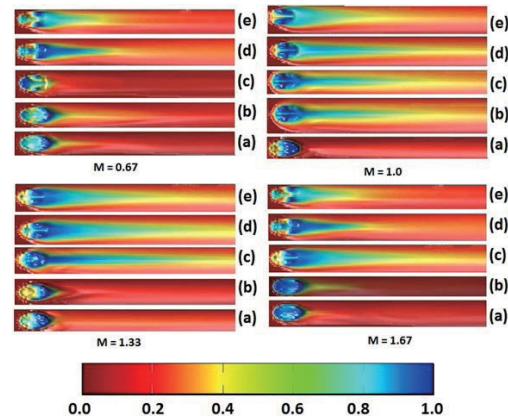


Fig. 27. Film cooling effectiveness contour at various blowing ratios for different hole shapes. In figure (a) Cylindrical (b) Semi-cylindrical (c) Triangular (d) Elliptic (e) Semi-elliptic

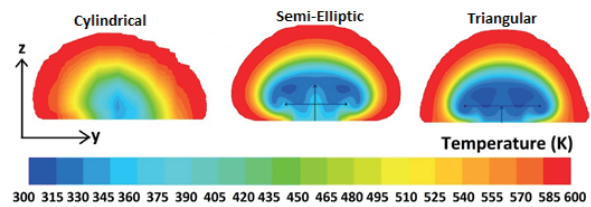


Fig. 28. Temperature contours on a cross-plane downstream of the location of coolant jet

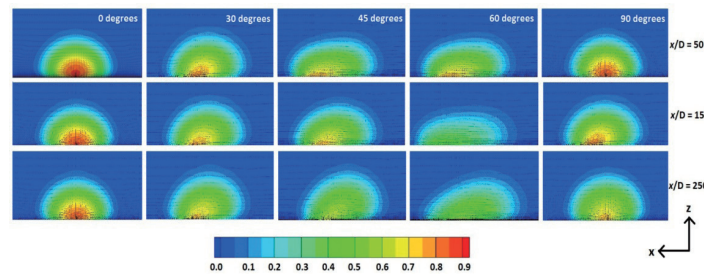


Fig. 29. Effectiveness contours for different orientations in the  $xz$  plane of the flow

surface resulting in higher overall effectiveness values than in the case with conventional Cylindrical hole.

The Fig. 29 shows the effectiveness contours for different orientations in the  $xz$  plane of the flow. The interactions of coolant jet core and the mainstream hot gases at three different locations on the  $xz$  plane can be seen from these contours. For less orientation angles, as the flow is moving towards the wall, effective penetration of the coolant jet in the downstream direction has been resulted which provides more effective spreading of coolant hence increasing the overall effectiveness. For the compound angles  $\beta = 0^\circ$  and  $\beta = 90^\circ$ , the penetration of the coolant jet is very high at  $x/D = 50$ , whereas at  $x/D = 250$ , the jet penetration is slightly less for  $\beta = 0^\circ$  but for  $\beta = 90^\circ$  orientations, the penetration becomes considerably less. It can also be seen from the figure, that the lateral spreading of the coolant jet shifts from right to left in the longitudinal direction with the change of orientations of holes (from  $\beta = 30^\circ$  to  $\beta = 60^\circ$ ).

## 5. Conclusions

Various hole shaped geometries (cylindrical, triangular; semi-cylindrical and semi-elliptic) have been presented and compared to each other for better results in terms of centreline & spatially averaged film cooling effectiveness. The triangular hole shape gave the highest film cooling effectiveness values at almost all the blowing ratios. This might be because of the geometry of the hole which increased the lateral spreading and gave reduced jet heights. While further it enhances the effectiveness upto 100% than the cylindrical hole shape. Reduced coolant jet height was observed for the triangular and semi-elliptic hole shapes which in turn resulted for higher centreline film cooling effectiveness. Also, the semi-elliptic hole shape is far more advantageous as the coolant mass flow rate is only half to that of as required by the cylindrical hole shape for the same blowing ratio. Higher effectiveness values are obtained because of the lowest

coolant jet heights in this case. Further adding the more number of rows of hole shapes gave better results. Out of the aligned and staggered rows of holes, later gave far better results in terms of film cooling effectiveness and coolant jet heights. The two staggered rows of semi-elliptic holes gave around twice the values of spatially averaged effectiveness than in the case of single row of cylindrical hole. The study of orientation of holes has also been carried out which showed that there is a significant increase of about 400% in the spatially averaged effectiveness from rows of semi-elliptic holes rather than the single row of cylindrical holes. Finally from the current study it can be recommended to use two numbers of staggered rows of semi-elliptic shaped holes for film cooling with a compound angle of  $90^\circ$  or  $0^\circ$  for better effectiveness with less coolant mass consumption.

## References

- [1] Abbe, A. and Jubran, B. A., "Numerical Modelling of Film Cooling from Converging Slot-hole", *Heat Mass Transfer Journal Springer*, Vol. 43, No. 4, 2007, pp. 381–388. DOI 10.1007/s00231-006-0115-9
- [2] Bunker, R. S., "A Review of Shaped Hole Turbine Film-cooling Technology," *ASME Journal of Heat Transfer*, Vol. 127, No. 4, 2005, pp. 441-453.
- [3] Goldstein, R. J., Eckert, E. R. G. and Ramsey, J. W., "Film Cooling with Injection through Holes: Adiabatic Wall Temperatures Downstream of a Circular Hole," *Journal of Engineering for Power*, Vol. 90, No. 4, 1968, pp. 384-393.
- [4] Goldstein, R. J., *Film Cooling*, Academic Press, Chapter-Advances in Heat Transfer, New York, 1971.
- [5] Yuen, C. H. N. and Martinez-Botas, R. F., "Film Cooling Characteristics of a Single Round Hole at Various Streamwise Angles in a Crossflow: Part I Effectiveness," *International Journal of Heat and Mass Transfer*, Vol. 46, 2003, pp. 221-235.
- [6] Yuen, C. H. N. and Martinez-Botas, R. F., "Film Cooling Characteristics of Rows of Round Holes at Various

Streamwise Angles in a Crossflow: Part II. Heat Transfer Coefficient”, *International Journal of Heat and Mass Transfer*, Vol.46, 2003, pp. 237-249.

[7] Wang, T. and Li, X., “Mist Film Cooling Simulation at Gas Turbine Operating Conditions”, *International Journal of Heat and Mass Transfer*, Vol. 51, 2008, pp. 5305-5317.

[8] Li, G., Zhu, H. and Fan, H., “Influence of Hole Shapes on Film Cooling Characteristics with CO<sub>2</sub> Injection”, *Chinese Journal of Aeronautics*, Vol. 21, 2008, pp. 393-401.

[9] Asghar, F. H. and Hyder, M. J., “Computational Study of Film Cooling Effectiveness for a Comparison of Cylindrical, Square and Triangular Holes of Equal Cross-Sectional Area”, *Mehran University Research Journal of Engineering & Technology*, Vol. 29, No. 4, 2010.

[10] Jindal, P., Roy, A. K. and Sharma, R. P., “Numerical Study of Film Cooling For Various Coolant Inlet Geometries”, *International Journal of Engineering and Technology (IJET)*, Vol. 7, No. 5, 2015, pp. 1659-1670.